A Comprehensive Screen of Metal Oxide Nanoparticles for DNA Adsorption, Fluorescence Quenching, and Anion Discrimination

Biwu Liu and Juewen Liu*

Department of Chemistry, Waterloo Institute for Nanotechnology,

University of Waterloo, Waterloo, Ontario, N2L 3G1, Canada

ABSTRACT

While DNA has been quite successful in metal cation detection, anion detectioin remains challenging due to the charge repulsion. Metal oxides represent a very important class of materials, and different oxides might interact with anions differently. In this work, a comprehensive screen of common metal oxide nanoparticles (MONPs) was carried out for their ability to adsorb DNA, quench fluorescence, and release adsorbed DNA in the presence of target anions. A total of 19 MONPs were studied, including Al_2O_3, CeO_2, CoO, Co_3O_4, Cr_2O_3, Fe_2O_3, Fe_3O_4, In_2O_3, ITO, Mn_2O_3, NiO, SiO_2, SnO_2, a-TiO_2 (anatase), r-TiO_2 (rutile), WO_3, Y_2O_3, ZnO, ZrO_2. These MONPs have different DNA adsorption affinity. Some adsorb DNA without quenching the fluorescence, while others strongly quench adsorbed fluorophores. They also display different affinity toward anions probed by DNA desorption. Finally CeO_2, Fe_3O_4, and ZnO were used to form a sensor array to discriminate phosphate, arsenate, and arsenite from the rest using linear discriminant analysis. This study not only provides a solution for anion discrimination using DNA as a signaling molecule, but also provides insights into the interface of metal oxides and DNA.

KEYWORDS: metal oxides, DNA, biosensors, arsenate, phosphate.

INTRODUCTION

DNA is highly attractive for designing hybrid materials due to its programmability, cost-effectiveness, ease of modification, and ability to recognize a broad range of analytes.[1-6] While DNA has been interfaced with metal and carbon-based nanomaterials,[6-9] limited work was carried out on metal oxide nanoparticles (MONPs).[10-20] MONPs represent a very important class of material due to their unique electronic, optical, magnetic and catalytic properties. DNA-functionalized MONPs might be useful as a sensor platform for anion detection. For example, when a fluorescently-labeled DNA is adsorbed by iron oxide nanoparticles, the fluorescence is quenched.[11] Arsenate adsorbs very strongly on iron oxide,[21-22] displacing adsorbed DNA and regaining fluorescence. We hypothesize that other metal oxides might have different adsorption affinity trends towards different anions, allowing their distinction using a sensor array. In this work, we screen a total of 19 MONPs with the intention to find distinct adsorption patterns as a general way for anion discrimination. While various pattern recognition methods have been reported,[23-30] this is the first based on MONPs.

Different MONPs may have different affinities with DNA. At the same time, they also adsorb anions differently. Such differences may allow a pattern-recognition-based sensor array for anion discrimination. Arsenic is a highly toxic heavy metalloid. Long-term exposure to even low concentrations of arsenic results in many adverse health effects, damaging the skin, heart, stomach, and nervous system.[31-34] Inorganic arsenic exists in two forms in water: As(V) (arsenate) and As(III) (arsenite). For environmental science, it is important to know arsenic speciation.[35] Detection of phosphate is important on its own. Most river water has a low phosphate level, and elevated phosphate leads to water eutrophication problems.[36] In this work, we aim to screen for different MONPs and detect phosphate, arsenate and arsenite.

MATERIALS AND METHODS

Chemicals. All of the DNA samples were from Integrated DNA Technologies (IDT, Coralville, IA, USA). Their sequences and modifications are FAM-24 mer (FAM-ACG CAT CTG TGA AGA GAA CCT GGG), FAM-A_{15} (FAM-AAA AAA AAA AAA AAA), FAM-T_{15} (FAM-TTT TTT TTT TTT TTT), and FAM-C_{15} (FAM-CCC CCC CCC CCC CCC). Metal oxide nanoparticles (MONPs) were purchased from Sigma or US Research Nano. The detailed information of the MONPs is shown in Table S1. Sodium fluoride, sodium chloride, sodium bromide, sodium iodide, sodium nitrate, sodium bicarbonate, sodium acetate, sodium citrate, sodium phosphate dibasic heptahydrate, and 4-(2-hydroxyethyl) piperazine-1-ethanesulfonic acid (HEPES) were from Mandel Scientific (Guelph, ON, Canada). Sodium (meta)arsenite, sodium arsenate dibasic heptahydrate, sodium sulfate, sodium sulfite and sodium perchlorate were purchased from Sigma. Sodium silicate solution (40 wt %) was from Ward's Science. Milli-Q water was used for all of the experiments.

Dynamic Light Scattering (DLS). The hydrodynamic size and ζ-potential of MONPs in the aqueous environment were measured using DLS (Zetasizer Nano 90, Malvern). Typically, 50 μg/mL of MONPs were dispersed in Milli-Q water for the size measurement or in HEPES buffer (10 mM, pH 7.6) for the ζ-potential measurement. To evaluate the effect of anion adsorption on surface charge, 0.5 mM of anions (phosphate, arsenate, arsenite, and silicate) were incubated with each MONP for 1 h before the measurement.

DNA Adsorption Capability of MONPs. To screen MONPs for effective DNA adsorption, 200 nM of FAM-24 mer DNA was mixed with different MONPs (0.5 mg/mL) in Buffer A (HEPES 10 mM, pH 7.6, NaCl 300 mM). After 2 h incubation, each MONP was centrifuged (CeO_2, 100,000 rpm for 10 min; other nanoparticles, 10,000 rpm for 10 min). The DNA/MONP conjugates were

prepared in a similar way for the following experiments unless otherwise indicated. The fluorescence images were taken using a digital camera under the 470 nm LED light excitation. The fluorescence intensity of the supernatant after adsorption was measured using a microplate reader (Infinite F200 Pro, Tecan; excitation: 485 nm, emission: 535 nm). The DNA adsorption on MONPs at low pH was performed using a similar procedure and the same DNA/particle ratio. pH was adjusted by adding HCl to a final of 10 mM. After 10 min incubation and centrifugation, the pH of supernatant was adjusted to neutral by adding NaOH (10 mM). Next, the fluorescence of supernatant was measured after dilution with Buffer A.

DNA Desorption by Anions. To measure the DNA displacement by anions, the DNA/MONP conjugate was firstly prepared using the method as described above. Typically, FAM-24 mer DNA (100 nM) was mixed with MONPs (CeO_2, 0.01 mg/mL; CoO, 0.25 mg/mL; Cr_2O_3, 0.25 mg/mL; Fe_2O_3, 0.1 mg/mL; Fe_3O_4, 0.15 mg/mL; In_2O_3, 0.4 mg/mL; Mn_2O_3, 0.4 mg/mL; NiO, 0.1 mg/mL; a-TiO_2, 0.1 mg/mL; and ZnO, 0.12 mg/mL) in Buffer A and the mixtures were incubated for 1 h. Afterwards, phosphate (1 mM) was introduced to the DNA/MONP conjugates. After another 1 h incubation and centrifugation, the fluorescence spectra from the supernatants were recorded. The fluorescence images of DNA/MONP in the presence of different anions (0.5 mM each) were taken using the camera under 470 nm light excitation.

Effect of DNA Sequence on Desorption. To evaluate the effect of DNA sequence on the signal enhancement, FAM A_{15}, T_{15}, or C_{15} (10 nM each) was incubated with five MONPs (Cr_2O_3, 0.05 mg/mL; In_2O_3, 0.05 mg/mL; Mn_2O_3, 0.03mg/mL; a-TiO_2, 0.03 mg/mL; and ZnO, 0.02 mg/mL) in Buffer A, respectively. Phosphate (50 μM) was added to induce fluorescence recovery. Desorption kinetics were recorded for 1 h. The fluorescence enhancement (F/F_0-1) was plotted as a function of DNA sequence.

Sensor Array for Anion Discrimination. The response of each sensor is plotted by the fluorescence enhancement (F/F_0-1) from different anions. The concentrations of MONPs and DNA are listed in Table S2. The concentration of target anions (PO_4^{3-}, As(V), and As(III)) was 10 μM, and all other anions was 1 mM. Target anions were replicated six times, and other anions were in triplicate. The fluorescence was recorded after adding the anions for 10 min. The training data were analyzed using canonical discriminate analysis from Origin.

RESULTS AND DISCUSSION

Rationale of Sensor Design. Our experiment design is described in Figure 1. We started with nineteen commercially available MONPs, covering early and later transition metals as well as lanthanides. The final candidates need to offer different adsorption affinities for these anions. At the same time, they need to adsorb DNA, quench adsorbed fluorophore and allow displacement of adsorbed DNA by target anions. Therefore, our screen of the MONPs is based on these criteria.

Screen for DNA Adsorption. We first screened the MONPs for DNA adsorption and fluorescence quenching. A FAM (6-carboxyfluorescein) labeled DNA (named FAM-24 mer) was incubated with each MONP at pH 7.6. The buffer also included 300 mM NaCl to screen electrostatic interactions. After centrifugation to precipitate the MONPs, the samples were observed under 470 nm excitation (Figure 2A). The supernatant in each sample was also measured using a microplate reader for quantification of DNA adsorption efficiency (Figure 2B). Little DNA adsorbed on Al_2O_3, SiO_2, SnO_2, WO_3 or ZrO_2. The rest of the MONPs adsorbed DNA to various degrees. To test whether the poor DNA adsorption by some MONPs is attributable to insufficient particle concentration, we also measured the DNA adsorption at a lower pH (pH adjusted with 10 mM HCl). MONPs are more protonated at lower pH and should bind negatively charged DNA more

tightly. Indeed, all the samples achieved quantitative DNA adsorption using the same amount of MONPs (Figure S1), indicating the lack of adsorption at pH 7.6 (e.g., Co_3O_4, and r-TiO_2) is not related to surface area. Since we intend to use the sensors at neutral pH, Al_2O_3, SiO_2, SnO_2, WO_3, ZrO_2, Co_3O_4, and r-TiO_2 were ruled out after this step of screening.

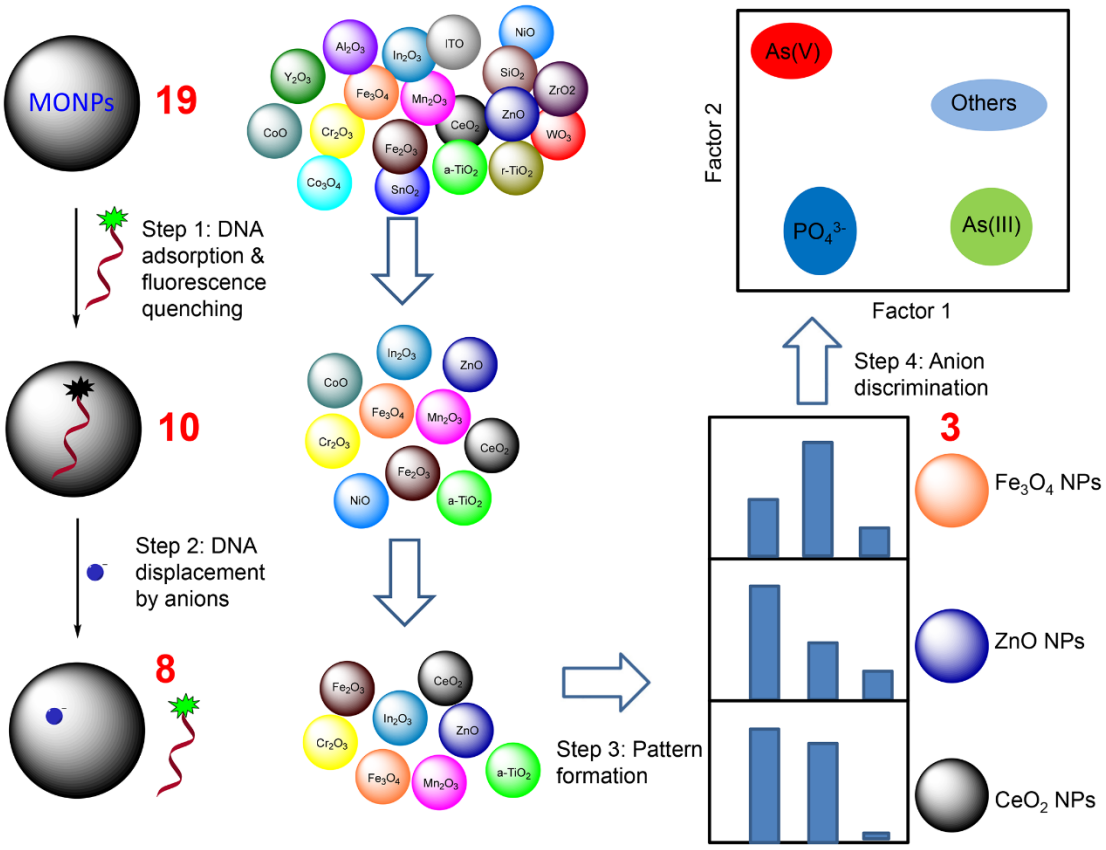

Figure 1. Schematic representation of the sensing strategy. Nineteen commercial MONPs were individually tested for adsorbing DNA and quenching fluorescence, from which eight were selected. These eight MONPs were tested with the different anions for DNA displacement, selectivity, and signaling. Finally, data from CeO_2, ZnO and Fe_3O_4 were used for discriminating arsenate, arsenate and phosphate using linear discriminant analysis. The numbers in red indicate the remaining number of MONPs after each screening step. The signaling scheme is included on the left side of the figure.

The remaining MONPs are divided into two groups. Most MONPs strongly quench fluorescence upon DNA adsorption as indicated by the dark pellets and dark supernatants in Figure 2A. The remaining four (In_2O_3, ITO, Y_2O_3, and ZnO) display fluorescent pellets and dark supernatant, indicating that these MONPs might be poor fluorescence quenchers. A low quenching efficiency is attributed to a large band gap and disfavored electron transfer (e.g., band gap of Y_2O_3 = 5.85 eV).[37-38] Among these four oxides, In_2O_3 can adsorb DNA and quench fluorescence better than ITO.[10] We are particularly concerned about Y_2O_3 and ZnO, since they can efficiently adsorb DNA and are potential good candidates for anions sensing. After dispersing in buffer, the quenching efficiency of ZnO and Y_2O_3 was quantified to be ~90% and ~50%, respectively (Figure S2). Since quenching is critical for our sensor design, Y_2O_3 and ITO were also ruled out. After this round of screening, only ten MONPs were left (Figure 1).

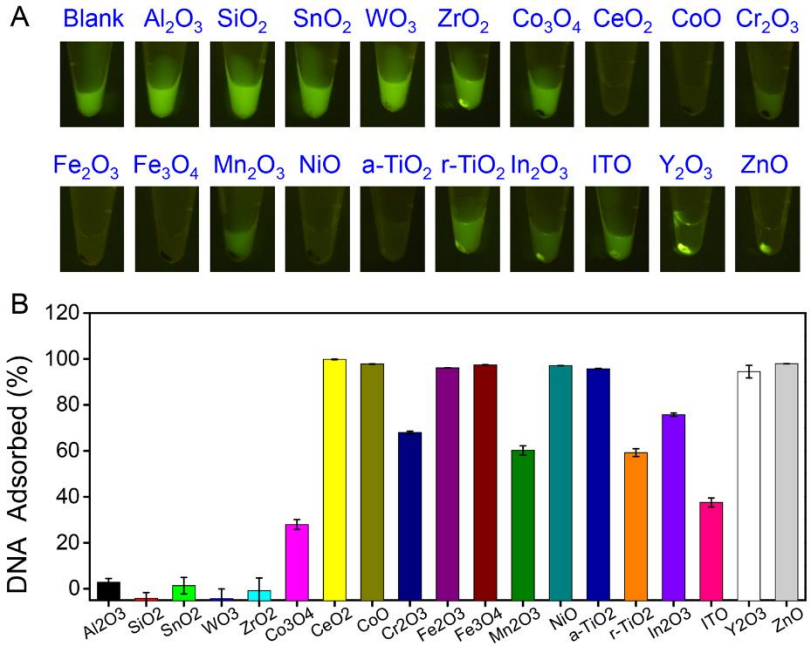

Figure 2. DNA adsorption and fluorescence quenching by various MONPs. The FAM-24 mer DNA (200 nM) is mixed with each MONP (0.5 mg/mL) in Buffer A (HEPES 10 mM, pH 7.6, 300

mM NaCl). (A) Photographs showing the samples under LED light excitation (470 nm) after centrifugation. Bright pellets indicate DNA adsorption with poor quenching, while bright supernatants indicate poor DNA adsorption. (B) Quantitative measurement of adsorbed DNA based on the free DNA remaining in the supernatant. The error bars represent the standard deviations from three independent measurements.

Screen for DNA Desorption. After efficient DNA probe adsorption and fluorescence quenching, the adsorbed probe needs to be displaced by target anions for signaling (see the left side of Figure 1 for the sensing scheme). Therefore, we next measured anion-induced DNA release using the remaining ten MONPs. For this experiment, we started with the free FAM-24 mer DNA, which displayed strong fluorescence (the black spectra in Figure 3). After adding each MONP, all the samples were quenched efficiently (the red spectra in Figure 3); this is consistent with our above screening results. Then 0.5 mM phosphate was added to each sample to induce DNA displacement (green spectra in Figure 3). The DNA on CoO and NiO was not displaced much by phosphate (less than 5%) and these two were ruled out for further studies (Figure 3B, 3H). It is likely that they interact too strongly with DNA. All other MONPs released the DNA probe upon adding phosphate, and they might be useful candidates for further biosensor development.

This displacement assay is also useful for understanding the interaction mechanism between DNA and MONPs. DNA has two structural elements for adsorption by surfaces: 1) negatively charged phosphate and 2) nucleobases. For metallic nanoparticles (e.g., AuNPs) and carbon-based nanomaterials (e.g., graphene oxide and carbon nanotubes), DNA adsorption is achieved mainly via base interaction.[8-9, 39-41] For example, adding phosphate has little effect on DNA adsorbed by these materials. Many MONPs (e.g., TiO_2, CeO_2, ITO) adsorb DNA mainly via the phosphate

backbone.[10, 12-14] Here, we confirmed that phosphate backbone binding is also important for DNA adsorption onto Cr_2O_3, Mn_2O_3 and ZnO.

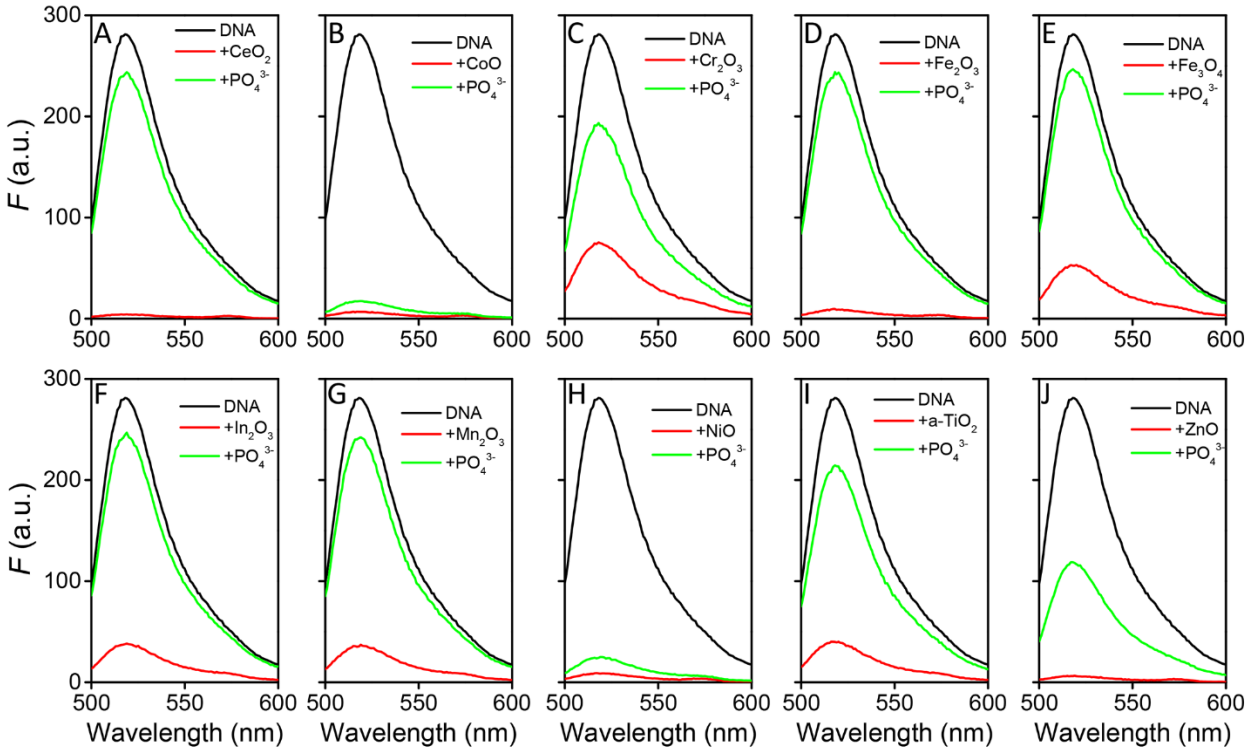

Figure 3. Phosphate-induced DNA release from (A) CeO_2, (B) CoO, (C) Cr_2O_3, (D) Fe_2O_3, (E) Fe_3O_4, (F) In_2O_3, (G) Mn_2O_3, (H) NiO, (I) a-TiO_2, and (J) ZnO. The ten MONPs were added to FAM-24 mer DNA (100 nM) in Buffer A to achieve fluorescence quenching (red spectra). After adding phosphate (0.5 mM) and centrifugation, the fluorescence spectra of the DNA in the supernatant were then measured (green spectra). The free DNA spectra are in black.

In addition to phosphate, we also tested DNA displacement by other common oxyanions: arsenate, arsenite, and silicate (Figure S3). They are all environmentally important analytes and may share a similar binding mechanism on MONPs. Interestingly, it is difficult to displace DNA from CoO and NiO using any of these anions. Other oxides allowed easier DNA displacement. Anion

adsorption was also confirmed by the ζ-potential change of MONPs (Figure S4). For example, the slightly negative charged CeO_2 (-4.23 ± 0.55 mV) becomes much more negative (~ 50 mV) after adsorbing oxyanions. The positive surface of ZnO becomes negative after adsorbing phosphate, arsenate, or arsenite.

While many MONPs enhanced fluorescence upon anion addition, they do so in a non-specific way; various anions can all produce fluorescence signal. Therefore, it is difficult to use single DNA/MONP complexes for selective anion detection, and the remaining eight MONPs were used to form a sensor array to solve the selectivity problem.

Sensor Optimization. After screening for DNA adsorption and desorption, we next optimized the signaling conditions. First, we evaluated the effect of DNA sequence. While the interaction between DNA and MONPs are mainly through the DNA phosphate backbone, DNA sequence may still be important due to possible secondary structures and weak base interactions. The previously used FAM-24 mer is a random DNA containing all the four types of nucleobases. We then compared FAM-A_{15}, FAM-T_{15}, and FAM-C_{15} as probes for signalling. FAM-G_{15} was not tested since poly-guanine strongly quenches fluorescence. A fixed concentration of phosphate (50 μM) was added to induce DNA desorption. The fold of fluorescence enhancement (F/F_0-1) is plotted for various MONPs (Figure 4A). Interestingly, DNA sequence indeed has a huge influence on sensor signaling. The DNA sequence induced the largest signal enhancement was chosen for further sensor development (i.e., A_{15} for Cr_2O_3; C_{15} for In_2O_3; T_{15} for Mn_2O_3, a-TiO_2, and ZnO). We did not study the other three MONPs here since they were optimized in previous work; the optimal sequences are T_{15} for CeO_2; and C_{15} for Fe_3O_4 and Fe_2O_3.[11-12] Therefore, DNA bases also appear to influence DNA adsorption and desorption.

For sensing applications, signaling kinetics are also a very important parameter and this was tested next (Figure 4B). After 4 min background fluorescence scan, phosphate was added and the kinetics of fluorescence increase were monitored. All the samples showed fast fluorescence recovery, achieving a plateau within 10 min (Figure 4B). Therefore, we quantified the fluorescence signal at 5 min after adding target anions for further investigation.

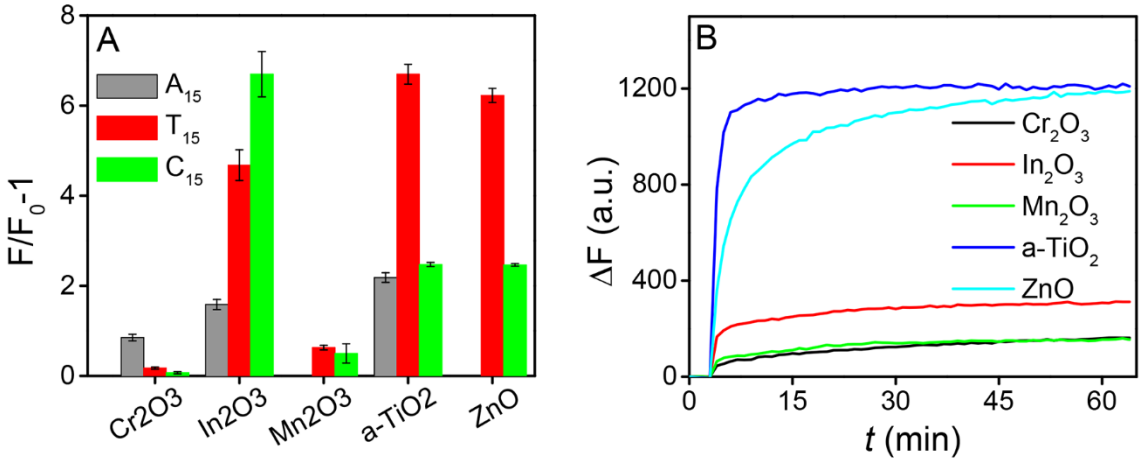

Figure 4. Optimization of (A) DNA sequence and (B) reaction time for different metal oxides. 15-mer DNA (poly-A, T, C) was incubated with five MONPs. Phosphate (50 μM) was used to induce fluorescence recovery.

Array-based Anion Sensing. After screening MONPs and optimizing DNA sequence, we next tested the sensor responses in the presence of various common anions. To obtain a training data set, each target anion (phosphate, arsenate, and arsenite) was repeated six times, and other anions were run in triplicates. As shown in Figure 5 and Figure S5-S9, each MONP shows a differential response to each target anion. As reported previously, DNA/Fe_3O_4 (Figure 5B) and Fe_2O_3 (Figure S7) have the strongest response to arsenate.[11] A main goal of this work is to screen for MONPs with preferred binding towards phosphate and arsenite. After several steps of screening, we indeed found MONPs with selectivity for phosphate over arsenate, including CeO_2 (Figure 5A), ZnO

(Figure 5C), Cr_2O_3 (Figure S5), In_2O_3 (Figure S8), and a-TiO_2 (Figure S9). However, other anions caused significant interference. For example, fluoride, carbonate, and sulfite resulted in even more DNA desorption than phosphate using Cr_2O_3. Carbonate also induced significant fluorescence enhancement in the Fe_2O_3 (Figure S7) and In_2O_3 samples (Figure S8). Furthermore, while Mn_2O_3 shows a slightly higher affinity to arsenite (Figure S6), bromide, nitrate, and sulfate also induce similar signal enhancement. Therefore, these MONPs were also ruled out and only three remained in this final step (the three shown in Figure 5A-C).

While the selectivity of each DNA/MONP sensor is limited, this difference might be large enough to form a pattern recognition based detection method. Our main goal is to identify phosphate, arsenate and arsenite. We chose to use an array formed by CeO_2, Fe_3O_4, and ZnO. They give selective responses to arsenate, arsenite and phosphate, while other anions do not produce much signal. Using this array, we first obtained a set of training data (Table S2). As a proof of concept, it is quite easy to separate these three anions from the rest using the canonical score plot (Figure 5D).

We previously reported the sensitivity of arsenate detection using Fe_3O_4 NPs, and phosphate showed a slightly lower response. However, the response of arsenite was much weaker. Here, we also measured the response of CeO_2/FAM-T_{15} complex to arsenite (Figure S10). The fluorescence linearly increased and a detection limit of 1.0 μM was obtained.

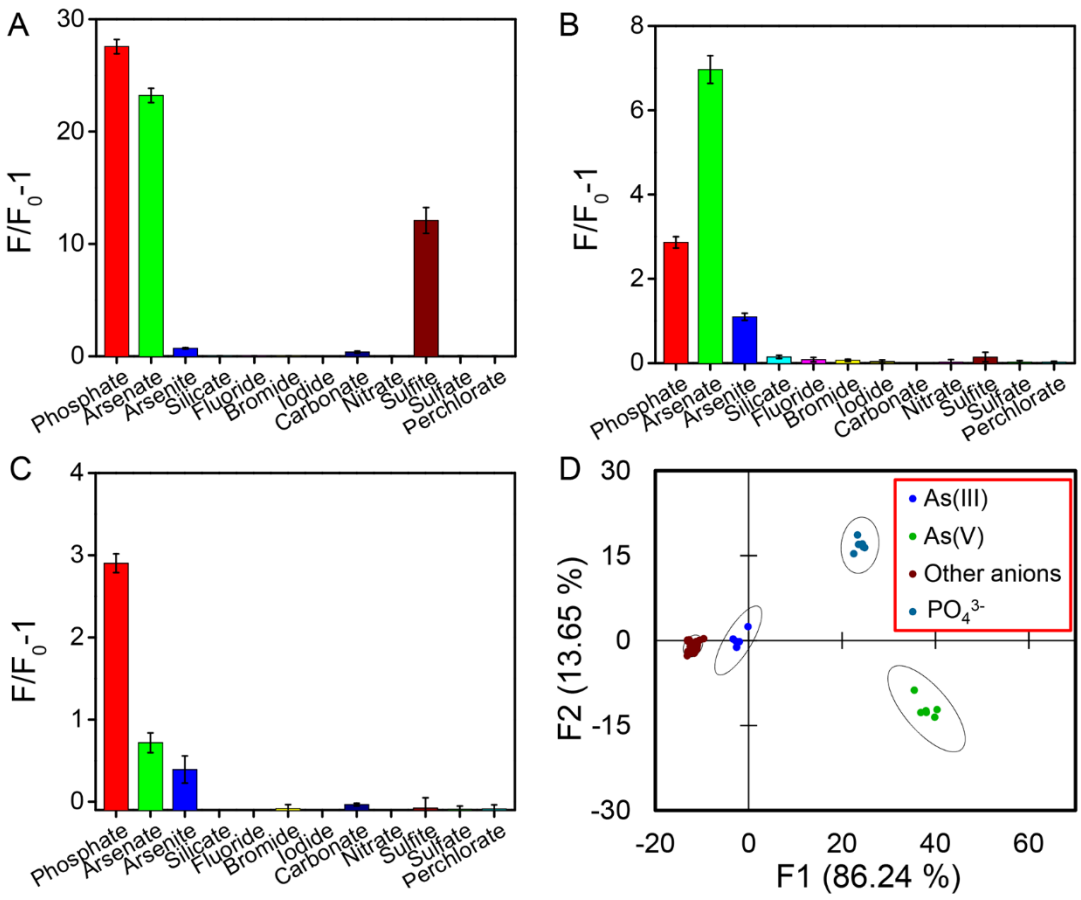

Figure 5. Signal enhancement of FAM-labeled DNA adsorbed onto (A) CeO_2, (B) Fe_3O_4, and (C) ZnO nanoparticles for various anions. The concentration of phosphate, arsenate, arsenite and silicate was 10 µM, and that of all other anions was 1 mM. Data for other MONPs are in Supporting Information. (D) The canonical score plot for fluorescence enhancement using three DNA/MONP (CeO_2, Fe_3O_4, and ZnO) sensors for the discrimination of phosphate, arsenate, and arsenite in the presence of interference anions. The 'other anions' include fluoride, bromide, iodide, silicate, carbonate, nitrate, sulfite, sulfate, and perchlorate.

CONCLUSIONS

In the past two decades, significant progresses have been made in DNA-based biosensors for metal cations and neutral molecules.[42-43] However, small anion detection remains difficult, since anions are repelled by negatively charged DNA, leading to poor interactions. This work demonstrates a large potential of using DNA plus MONPs for anion sensing. We screened nineteen types of common MONPs for their DNA adsorption, fluorescence quenching, and anion-induced DNA displacement property. Based on the anion selectivity pattern, we chose to use CeO_2, Fe_3O_4, and ZnO to form a sensor array, which successfully discriminated phosphate, arsenate, and arsenite from other common anions. This study provides a comprehensive understanding on the interaction between DNA and metal oxides, and the influence of environmentally important analytes on DNA adsorption.

ASSOCIATED CONTENT

Supporting Information

Additional DNA adsorption data, zeta-potential, and anion response data.

AUTHOR INFORMATION

Corresponding Author

*Fax: (+1) 519-746-0435 E-mail: liujw@uwaterloo.ca.

Notes

The authors declare no competing financial interest.

ACKNOWLEDGMENTS

Funding for this work is from the NSERC of Canada (Discovery and Strategic Project Grant: STPGP-447472-2013 055766).

REFERENCES

(1) Wang, H.; Yang, R.; Yang, L.; Tan, W. Nucleic Acid Conjugated Nanomaterials for Enhanced Molecular Recognition. *ACS Nano* **2009,** *3,* 2451-2460.

(2) Li, D.; Song, S.; Fan, C. Target-Responsive Structural Switching for Nucleic Acid-Based Sensors. *Acc. Chem. Res.* **2010,** *43,* 631-641.

(3) Katz, E.; Willner, I. Nanobiotechnology: Integrated Nanoparticle-Biomolecule Hybrid Systems: Synthesis, Properties, and Applications. *Angew. Chem., Int. Ed.* **2004,** *43,* 6042-6108.

(4) Zhao, W.; Brook, M. A.; Li, Y. Design of Gold Nanoparticle-Based Colorimetric Biosensing Assays. *ChemBioChem* **2008,** *9,* 2363-2371.

(5) Tan, W.; Donovan, M. J.; Jiang, J. Aptamers from Cell-Based Selection for Bioanalytical Applications. *Chem. Rev.* **2013,** *113,* 2842-2862.

(6) Rosi, N. L.; Mirkin, C. A. Nanostructures in Biodiagnostics. *Chem. Rev.* **2005,** *105,* 1547-1562.

(7) Liu, J.; Cao, Z.; Lu, Y. Functional Nucleic Acid Sensors. *Chem. Rev.* **2009,** *109,* 1948-1998.

(8) Liu, J. Adsorption of DNA onto Gold Nanoparticles and Graphene Oxide: Surface Science and Applications. *Phys. Chem. Chem. Phys.* **2012,** *14,* 10485-10496.

(9) Li, F.; Pei, H.; Wang, L.; Lu, J.; Gao, J.; Jiang, B.; Zhao, X.; Fan, C. Nanomaterial-Based Fluorescent DNA Analysis: A Comparative Study of the Quenching Effects of Graphene Oxide, Carbon Nanotubes, and Gold Nanoparticles. *Adv. Funct. Mater.* **2013,** *23,* 4140-4148.

(10) Liu, B.; Liu, J. DNA Adsorption by Indium Tin Oxide Nanoparticles. *Langmuir* **2015,** *31,* 371-377.

(11) Liu, B.; Liu, J. DNA Adsorption by Magnetic Iron Oxide Nanoparticles and Its Application for Arsenate Detection. *Chem. Commun.* **2014,** *50,* 8568-8570.

(12) Liu, B.; Sun, Z.; Huang, P.-J. J.; Liu, J. Hydrogen Peroxide Displacing DNA from Nanoceria: Mechanism and Detection of Glucose in Serum. *J. Am. Chem. Soc.* **2015,** *137,* 1290-1295.

(13) Pautler, R.; Kelly, E. Y.; Huang, P.-J. J.; Cao, J.; Liu, B.; Liu, J. Attaching DNA to Nanoceria: Regulating Oxidase Activity and Fluorescence Quenching. *ACS Appl. Mater. Interfaces* **2013,** *5,* 6820-6825.

(14) Zhang, X.; Wang, F.; Liu, B.; Kelly, E. Y.; Servos, M. R.; Liu, J. Adsorption of DNA Oligonucleotides by Titanium Dioxide Nanoparticles. *Langmuir* **2014,** *30,* 839-845.

(15) Feuillie, C.; Sverjensky, D. A.; Hazen, R. M. Attachment of Ribonucleotides on α-Alumina as a Function of pH, Ionic Strength, and Surface Loading. *Langmuir* **2015,** *31,* 240-248.

(16) Fan, H.; Zhao, Z.; Yan, G.; Zhang, X.; Yang, C.; Meng, H.; Chen, Z.; Liu, H.; Tan, W. A Smart DNAzyme–MnO2 Nanosystem for Efficient Gene Silencing. *Angew. Chem., Int. Ed.* **2015,** *54,* 4801-4805.

(17) Yuan, Y.; Wu, S.; Shu, F.; Liu, Z. An MnO_2 Nanosheet as a Label-Free Nanoplatform for Homogeneous Biosensing. *Chem. Commun.* **2014,** *50,* 1095-1097.

(18) Fahrenkopf, N. M.; Rice, P. Z.; Bergkvist, M.; Deskins, N. A.; Cady, N. C. Immobilization Mechanisms of Deoxyribonucleic Acid (DNA) to Hafnium Dioxide (HfO_2) Surfaces for Biosensing Applications. *ACS Appl. Mater. Interfaces* **2012,** *4,* 5360-5368.

(19) Suzuki, H.; Amano, T.; Toyooka, T.; Ibuki, Y. Preparation of DNA-Adsorbed TiO_2 Particles with High Performance for Purification of Chemical Pollutants. *Environ. Sci. Technol.* **2008,** *42,* 8076-8082.

(20) Fan, Y.; Chen, X.; Kong, J.; Tung, C.-h.; Gao, Z. Direct Detection of Nucleic Acids by Tagging Phosphates on Their Backbones with Conductive Nanoparticles. *Angew. Chem.* **2007,** *119,* 2097-2100.

(21) Liu, F.; De Cristofaro, A.; Violante, A. Effect of pH, Phosphate and Oxalate on the Adsorption/Desorption of Arsenate on/from Goethite. *Soil Sci.* **2001,** *166,* 197-208.

(22) Goldberg, S.; Johnston, C. T. Mechanisms of Arsenic Adsorption on Amorphous Oxides Evaluated Using Macroscopic Measurements, Vibrational Spectroscopy, and Surface Complexation Modeling. *J. Colloid Interface Sci.* **2001,** *234*, 204-216.

(23) Rakow, N. A.; Suslick, K. S. A Colorimetric Sensor Array for Odour Visualization. *Nature* **2000,** *406*, 710-713.

(24) Carey, J. R.; Suslick, K. S.; Hulkower, K. I.; Imlay, J. A.; Imlay, K. R. C.; Ingison, C. K.; Ponder, J. B.; Sen, A.; Wittrig, A. E. Rapid Identification of Bacteria with a Disposable Colorimetric Sensing Array. *J. Am. Chem. Soc.* **2011,** *133,* 7571-7576.

(25) De, M.; Rana, S.; Akpinar, H.; Miranda, O. R.; Arvizo, R. R.; Bunz, U. H. F.; Rotello, V. M. Sensing of Proteins in Human Serum Using Conjugates of Nanoparticles and Green Fluorescent Protein. *Nat. Chem.* **2009,** *1,* 461-465.

(26) Tan, S. S.; Kim, S. J.; Kool, E. T. Differentiating between Fluorescence-Quenching Metal Ions with Polyfluorophore Sensors Built on a DNA Backbone. *J. Am. Chem. Soc.* **2011,** *133,* 2664-2671.

(27) Kwon, H.; Jiang, W.; Kool, E. T. Pattern-Based Detection of Anion Pollutants in Water with DNA Polyfluorophores. *Chem. Sci.* **2015,** *6,* 2575-2583.

(28) Tao, Y.; Ran, X.; Ren, J.; Qu, X. Array-Based Sensing of Proteins and Bacteria By Using Multiple Luminescent Nanodots as Fluorescent Probes. *Small* **2014,** *10,* 3667-3671.

(29) Pei, H.; Li, J.; Lv, M.; Wang, J.; Gao, J.; Lu, J.; Li, Y.; Huang, Q.; Hu, J.; Fan, C. A Graphene-Based Sensor Array for High-Precision and Adaptive Target Identification with Ensemble Aptamers. *J. Am. Chem. Soc.* **2012,** *134,* 13843-13849.

(30) Ran, X.; Pu, F.; Ren, J.; Qu, X. A CuS-Based Chemical Tongue Chip for Pattern Recognition of Proteins and Antibiotic-Resistant Bacteria. *Chem. Commun.* **2015,** *51,* 2675-2678.

(31) Mandal, B. K.; Suzuki, K. T. Arsenic Round the World: A Review. *Talanta* **2002,** *58,* 201-235.

(32) Shen, S.; Li, X.-F.; Cullen, W. R.; Weinfeld, M.; Le, X. C. Arsenic Binding to Proteins. *Chem. Rev.* **2013,** *113,* 7769-7792.

(33) Charoensuk, V.; Gati, W. P.; Weinfeld, M.; Le, X. C. Differential Cytotoxic Effects of Arsenic Compounds in Human Acute Promyelocytic Leukemia Cells. *Toxicol. Appl. Pharmacol.* **2009,** *239,* 64-70.

(34) Cohen, S. M.; Ohnishi, T.; Arnold, L. L.; Le, X. C. Arsenic-Induced Bladder Cancer in an Animal Model. *Toxicol. Appl. Pharmacol.* **2007,** *222,* 258-263.

(35) Clancy, T. M.; Hayes, K. F.; Raskin, L. Arsenic Waste Management: A Critical Review of Testing and Disposal of Arsenic-Bearing Solid Wastes Generated during Arsenic Removal from Drinking Water. *Environ. Sci. Technol.* **2013,** *47,* 10799-10812.

(36) Warwick, C.; Guerreiro, A.; Soares, A. Sensing and Analysis of Soluble Phosphates in Environmental Samples: A Review. *Biosens. Bioelectron.* **2013,** *41,* 1-11.

(37) Zhang, H.; Ji, Z.; Xia, T.; Meng, H.; Low-Kam, C.; Liu, R.; Pokhrel, S.; Lin, S.; Wang, X.; Liao, Y.-P.; Wang, M.; Li, L.; Rallo, R.; Damoiseaux, R.; Telesca, D.; Mädler, L.; Cohen, Y.; Zink, J. I.; Nel, A. E. Use of Metal Oxide Nanoparticle Band Gap To Develop a Predictive Paradigm for Oxidative Stress and Acute Pulmonary Inflammation. *ACS Nano* **2012,** *6,* 4349-4368.

(38) Koziej, D.; Lauria, A.; Niederberger, M. 25th Anniversary Article: Metal Oxide Particles in Materials Science: Addressing All Length Scales. *Adv. Mater.* **2014,** *26,* 235-257.

(39) Herne, T. M.; Tarlov, M. J. Characterization of DNA Probes Immobilized on Gold Surfaces. *J. Am. Chem. Soc.* **1997,** *119,* 8916-8920.

(40) Tu, X.; Manohar, S.; Jagota, A.; Zheng, M. DNA Sequence Motifs for Structure-Specific Recognition and Separation of Carbon Nanotubes. *Nature* **2009,** *460,* 250-253.

(41) Zhang, X.; Servos, M. R.; Liu, J. Surface Science of DNA Adsorption onto Citrate-Capped Gold Nanoparticles. *Langmuir* **2012,** *28,* 3896-3902.

(42) Famulok, M.; Hartig, J. S.; Mayer, G. Functional Aptamers and Aptazymes in Biotechnology, Diagnostics, and Therapy. *Chem. Rev.* **2007,** *107,* 3715-3743.

(43) Zhang, X.-B.; Kong, R.-M.; Lu, Y. Metal Ion Sensors Based on DNAzymes and Related DNA Molecules. *Annu. Rev. Anal. Chem.* **2011,** *4,* 105-128.